Cooperative Position-based Formation-pursuit of Moving Targets by Multi-UAVs with Collision Avoidance

Siti Nurjanah
Department of Electrical Engineering
Institut Teknologi Sepuluh Nopember
Surabaya, Indonesia
sitinurjanah180495@gmail.com

Trihastuti Agustinah
Department of Electrical Engineering
Institut Teknologi Sepuluh Nopember
Surabaya, Indonesia
trihastuti@ee.its.ac.id

Muhammad Fuad
Faculty of Electrical Engineering
Universitas Trunojoyo Madura
Bangkalan, Indonesia
fuad@trunojoyo.ac.id

***Abstract*— The process for capturing a moving target from searcher UAVs that move from their initial position until they encircle the target successfully while maintaining safety has to be supported by an integrated target capture strategy. This paper proposes an integrated target capture strategy that consists of dynamic task allocation, formation-pursuit using position-based strategy, and optimized artificial potential field (APF). A dynamic task allocation algorithm is used in 3D dynamic environments to allocate the target to several existing UAVs efficiently. Target information is disseminated to neighbor UAVs by the temporary leader of UAVs. For the formation-pursuit using a position-based strategy, destination points to create formation are made at the sphere coordinates around a moving target. The destination points are tracked using a fuzzy state feedback controller. An optimized APF algorithm is used to avoid collisions with targets, other UAVs, and static obstacles. Each UAV can choose the optimal trajectory to avoid obstacles and reset the formation after passing them. The simulation results show that multi-UAVs successfully surrounded and formed formation-pursuit of a moving target without colliding with the closest Euclidean distance between UAVs of 1.32957 m, UAVs with a target is 1.94359 m, and UAVs with static obstacles within a range of 1.60632 m.**

Keywords—formation-pursuit, multi-UAVs, obstacle avoidance, task allocation, tracking control.

I. INTRODUCTION

In recent years, quadcopter UAV has attracted considerable attention due to the large-scale applications that can be applied to both the military and civilian fields. The interest in this quadcopter UAV is due to its maneuverability, low cost, and ability to perform complex tasks in complex environments. Research on multi-UAV collaboration has been extensively developed to overcome the limitations of developing complex work environments, multiple tasks, and the performance of single UAVs. The implementation of multi-UAVs collaboration includes formation [1–3], flocking [4], target detection and tracking [5–7], task allocation [8–10], patrol and surveillance [11], [12], target encirclement [3], [13], [14] and collision avoidance [15], [16].

The research mentioned in the first paragraph shows that many researchers only focus on one problem, such as target tracking, task allocation, target encirclement, and collision avoidance. It is rare for researchers to combine several problems into one interconnected system. For example, research [10] examined a set of robots that disperse to find moving targets, where each target must be surrounded by more than two robots while considering security aspects. Multiple problems have been merged in this research. However, it was still applied to mobile robot systems. Based on the idea, this research aims to integrate multiple problems into an interrelated target capture strategy applied to multi-UAV by ensuring UAVs to avoid other UAVs and buildings.

A target capture strategy is designed for task allocation, forming a formation-pursuit, and conducting collision avoidance. The task allocation algorithm of UAVs is adopted from [10], which was previously used for a mobile robot. Furthermore, each UAV is assigned to surround the target by creating a formation-pursuit based on a position-based strategy. This strategy is based on generating points around the spherical coordinates of a moving target. These points become the reference positions for the UAVs. A fuzzy state feedback controller is utilized for tracking these desired positions, and the optimized APF from [15] is applied for safety purposes to ensure no collisions between UAVs, targets, and obstacles during capture.

This paper investigates fuzzy state feedback controls designed to track a moving target. This controller id designed for the quadcopter able to track a moving target. A scenario is created where multiple UAVs and a moving target are set in a dynamic 3D environment. The speed and position of the target are available when it enters the UAV's detection range. This information can also be obtained from neighboring UAVs.

The main contribution to this paper is to combine several different problems. The allocation of several UAVs to a moving target, formation-pursuit at sphere coordinate formed after tracking the desired position and generating a collision-free path during the target capture are three problems investigated in this research. In addition, this paper proposed fuzzy state feedback to track the target and optimal APF to guide UAVs to avoid obstacles.

The rest of this paper is organized as follows. Section II describes methods, including the quadcopter model, tracking control, dynamic task allocation, formation-pursuit scenario, and collision avoidance algorithm. Section III explains simulation results, and Section IV concludes this paper.

How to cite: Nurjanah, S., Agustinah, T., & Fuad, M. (2022). Cooperative Position-based Formation-pursuit of Moving Targets by Multi-UAVs with Collision Avoidance. *JAREE (Journal on Advanced Research in Electrical Engineering), 6*(2).

II. Material and Methods

A. Quadcopter Dynamics

This section presents a quadcopter dynamics model like those previously presented in [17]. Quanser Qdrone is the type of quadcopter used in this study (see Fig. 1).

Fig. 1. Quanser Qdrone [18]

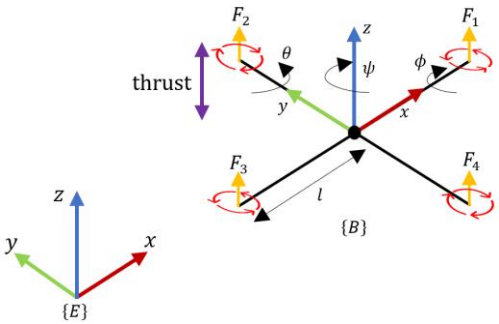

Fig. 2. Quadcopter configuration

TABLE I. Parameter of Quanser Qdrone [17]

Parameter	Symbol	Value
Mass (kg)	m	1
Gravity (m/ s^2)	g	9.81
Inertia moment of the X-axis (kg.m^2)	J_{xx}	0.03
Inertia moment of the Y-axis (kg.m^2)	J_{yy}	0.03
Inertia moment of the Z-axis (kg.m^2)	J_{zz}	0.04
Distance between rotor and center of mass (m)	l	0.2
Drag force (N)	d	3.13x10^{-5}

The quadcopter dynamics model is derived by introducing two frames involved, the earth and body frame (see Fig. 2). Refers to the translational motion model is derived from the earth frame (E -frame). It is related to the position $[X \quad Y \quad Z]^{\mathrm{T}}$ and velocity $[\dot{X} \quad \dot{Y} \quad \dot{Z}]^{\mathrm{T}}$ of the quadcopter in the earth frame. The rotational motion is derived from the body frame (B-frame) since it is related to the quadcopter movement itself. A rotational motion's roll (ϕ), pitch (θ), and yaw (ψ) angles in the body frame with the angular velocity equal to $[\dot{\phi} \quad \dot{\theta} \quad \dot{\psi}]^{\mathrm{T}}$.

Based on the previous studies, the quadcopter dynamics model can be written as follows:

$$\ddot{X} = (\sin\psi \sin\phi + \cos\psi \sin\theta \cos\phi)\frac{U_1}{m} \quad (1)$$

$$\ddot{Y} = (-\cos\psi \sin\phi + \sin\psi \sin\theta \cos\phi)\frac{U_1}{m} \quad (2)$$

$$\ddot{Z} = -g + (\cos\theta \cos\phi)\frac{U_1}{m} \quad (3)$$

$$\dot{p} = \frac{J_{yy}-J_{zz}}{J_{xx}} qr + \frac{U_2 l}{J_{xx}} \quad (4)$$

$$\dot{q} = \frac{J_{zz}-J_{xx}}{J_{yy}} pr + \frac{U_3 l}{J_{yy}} \quad (5)$$

$$\dot{r} = \frac{J_{xx}-J_{yy}}{J_{zz}} pq + \frac{U_4 d}{J_{zz}} \quad (6)$$

where $[p \quad q \quad r]^{\mathrm{T}} = [\dot{\phi} \quad \dot{\theta} \quad \dot{\psi}]^{\mathrm{T}}$ describes the angular velocities of a quadcopter, and $U_i(i = 1,2,3,4)$ represents the input controls. The parameter of Quanser Qdrone can be seen in Table I.

B. Proposed Tracking Control

A fuzzy state feedback controller is used for controlling the quadcopter's movements from the UAV's current position to the intended target point, then herding the besieged target towards the confinement area in a 3D environment. The state feedback controller manages the altitude (Z) and heading (ψ). A combination of state feedback controller and Sugeno-type fuzzy logic controller manages position XY and attitude $\phi\theta$. In this quadcopter tracking control, there is an inner loop for attitude control and an outer loop for position control.

1) Position Control

The fuzzy controller is used to control the 2D positions $[X \quad Y]^{\mathrm{T}}$. Those outputs of fuzzy controller are reference inputs for attitude control of ϕ and θ. In this study, the fuzzy controller had two inputs: distance and velocity from the quadcopter to the target. The output is the angle of the quadcopter.

Input

- Distance: The difference between the position (X and Y) of the quadcopter and the target. Membership of distance can be seen in **Error! Reference source not found.**.
- Velocity: The difference between the velocity ($\dot{X}$ and $\dot{Y}$) of the quadcopter and the target. Membership of velocity is indicated in Fig. 4.

Output

As seen in **Error! Reference source not found.**, the desired output ($s_{7_{ref}}$ and $s_{8_{ref}}$) becomes the input for the attitude controller (ϕ and θ), where the output value is $-0.5 < ref < 0.5$. It is assumed that the maximum slope UAV is 30°.

Rule Base

- If distance is far, then ref is 0.5
- If distance is middle and velocity is fast, then ref is 0.3
- If distance is close and velocity is fast, then ref is -0.5
- If distance is close and velocity is slow, then ref is 0

The altitude control (Z) using state feedback control, (3) modified by adding drag force to the state equation so that it becomes:

$$\ddot{Z} = -g + (\cos\theta \cos\phi)\frac{U_1}{m} - d.\dot{Z} \quad (7)$$

where

$$U_1 = \frac{m}{\cos\phi\cos\theta}\left(g + K_1\left(Z_{ref} - Z\right) + L_1\left(\dot{Z}_{ref} - \dot{Z}\right) + \ddot{Z}_{ref} + d.\dot{Z}\right) \quad (8)$$

So, if (8) is substituted to (7), then the $\ddot{Z}$ state equation becomes:

$$\ddot{Z} = K_1\left(Z_{ref} - Z\right) + L_1\left(\dot{Z}_{ref} - \dot{Z}\right) + \ddot{Z}_{ref} \quad (9)$$

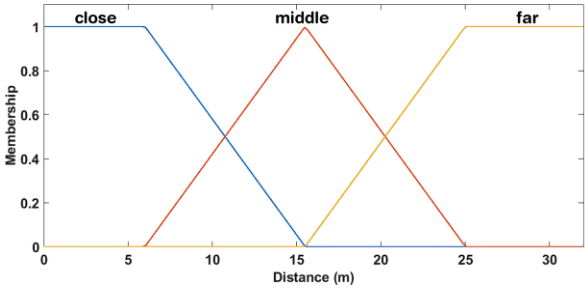

Fig. 3. Distance fuzzy input

The simplification (9) will simplify the control process because it only needs to find the K_1 and L_1 parameters that produce the best output.

2) Attitude Control

The quadcopter heading (ψ) is controlled using a state feedback control so that the value of $\psi \to 0$, with:

$$U_4 = \frac{Jzz}{d}\left(-K_4\psi - L_4\dot{\psi}\right) \quad (10)$$

Next, (10) is substituted into (6) so that it becomes:

$$\dot{r} = \frac{Jxx - Jyy}{Jzz}pq - K_4\psi - L_4\dot{\psi} \quad (11)$$

Since it is known from Table I, that the value of $J_{xx} = J_{yy}$, then (11) can be simplified to:

$$\dot{r} = -K_4\psi - L_4\dot{\psi} \quad (12)$$

Because of heading (ψ) was controlled by regulatory state feedback control, the value of $\psi \to 0$, so that (1) can be simplified to:

$$\ddot{X} = (\sin(0)\sin\phi + \cos(0)\sin\theta\cos\phi)\frac{U_1}{m}$$

where $\sin(0) = 0, \cos(0) = 1$, so

$$\ddot{X} = (s_7)\frac{U_1}{m} \quad (13)$$

where

$$s_7 = \sin\theta\cos\phi$$

From **Error! Reference source not found.**, s_7 is a variable controlled by using a state feedback controller to obtain a roll value (ϕ). The derivative of s_7 is assumed to be equal to p, thus becoming:

$$\dot{s}_7 \approx p$$
$$\ddot{s}_7 \approx \dot{p} = \frac{J_{yy} - J_{zz}}{J_{xx}}qr + \frac{U_2 l}{J_{xx}} \quad (14)$$

Subsequently, U_2 on **Error! Reference source not found.** is modified to:

$$U_2 = \frac{Jxx}{l}\left(K_2 s_{7_{ref}} - K_2 s_7 - L_2\dot{s}_{7_{ref}} - L_2\dot{s}_7 + \ddot{s}_{7_{ref}}\right) \quad (15)$$

So, if (15) is substituted to **Error! Reference source not found.**, then it becomes:

$$\ddot{s}_7 \approx \dot{p} = \frac{Jyy - Jzz}{Jxx}qr + K_2 s_{7_{ref}} - K_2 s_7 - L_2\dot{s}_{7_{ref}} - L_2\dot{s}_7 + \ddot{s}_{7_{ref}} \quad (16)$$

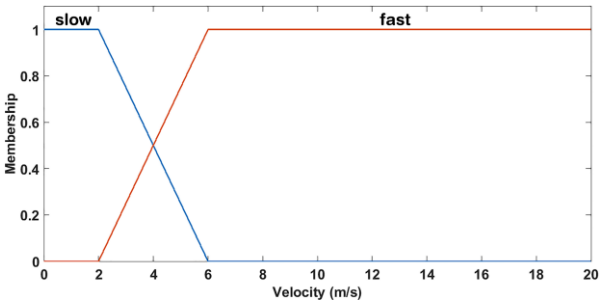

Fig. 4. Velocity fuzzy input

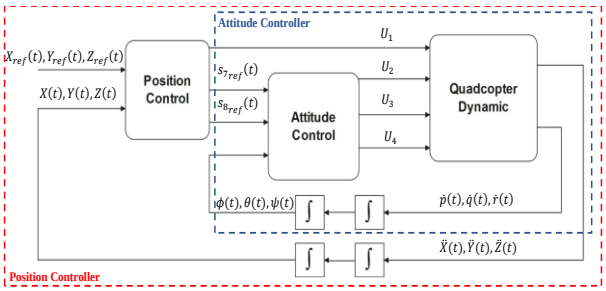

Fig. 5. Block diagram of tracking control

From Table I, it can be seen that the values of J_{yy} and J_{zz} have a very slight difference, so it can be considered zero. Then (16) can be simplified to:

$$\ddot{s}_7 \approx \dot{p} = K_2 s_{7_{ref}} - K_2 s_7 - L_2\dot{s}_{7_{ref}} - L_2\dot{s}_7 + \ddot{s}_{7_{ref}} \quad (17)$$

Similar to the previous step on position control X, (2) can be simplified to:

$$\ddot{Y} = (-\cos(0)\sin\phi + \sin(0)\sin\theta\cos\phi)\frac{U_1}{m}, \quad \sin(0) = 0, \cos(0) = 1$$
$$\ddot{Y} = -s_8\frac{U_1}{m} \quad (18)$$

where

$$s_8 = \sin\phi$$

From (18), s_8 is a variable controlled by using state feedback controller to obtain a pitch value (θ), where the derivative of s_8 is assumed to be equal to q, thus becoming:

$$\dot{s}_8 \approx q$$
$$\ddot{s}_8 \approx \dot{q} = \frac{J_{zz} - J_{xx}}{J_{yy}}pr + \frac{U_3 l}{J_{yy}} \quad (19)$$

Next, U_3 on (19) is modified to:

$$U_3 = \frac{Jyy}{l}\left(K_3 s_{8_{ref}} - K_3 s_8 - L_3\dot{s}_{8_{ref}} - L_3\dot{s}_8 + \ddot{s}_{8_{ref}}\right) \quad (20)$$

TABLE II. PARAMETER OF STATE FEEDBACK CONTROL

Parameter	Value	Parameter	Value
K_1	16	L_1	9
K_2	100	L_2	21
K_3	100	L_3	21
K_4	0.09	L_4	0.61

So, if (20) is substituted to (19), then it becomes:

$$\ddot{s}_8 \approx \dot{q} = \frac{J_{zz}-J_{xx}}{J_{yy}} pr + K_3 s_{8_{ref}} - K_3 s_8 - L_3 \dot{s}_{8_{ref}} - L_3 \dot{s}_8 + \ddot{s}_{8_{ref}} \quad (21)$$

From Table I, it is known that the values of J_{xx} and J_{zz} have a very small difference, so that it can be considered to be zero, then (21) can be simplified to:

$$\ddot{s}_8 \approx \dot{q} = K_3 s_{8_{ref}} - K_3 s_8 - L_3 \dot{s}_{8_{ref}} - L_3 \dot{s}_8 + \ddot{s}_{8_{ref}} \quad (22)$$

In attitude control of ϕ and θ, the state feedback controller requires the reference inputs $\left(s_{7_{ref}},\ \dot{s}_{7_{ref}},\ \ddot{s}_{7_{ref}},\ s_{8_{ref}},\ \dot{s}_{8_{ref}},\ \ddot{s}_{8_{ref}}\right)$ to get the desired ϕ and θ values. These reference values are the results of the output of the fuzzy controller.

The block diagram for the overall tracking control for each UAV can be seen in **Error! Reference source not found.**. The parameter values of the state feedback controller (K and L are positive constants) for (9), (10), (15), and (20) are obtained through trial and error by providing the intended waypoints/targets. The parameters can be used when the UAV reaches all the specified target points (see Table II).

C. Dynamic Task Allocation

In this study, a distributed algorithm is introduced for task allocation, where there is one moving target, and the target has to be surrounded by multiple UAVs. The dynamic task allocation algorithm is used to solve the problem of targeting capture by multi-UAVs. This algorithm is inspired by market and society mechanisms [19], which precisely describe negotiating and coordinating relationships between UAVs. In this dynamic task allocation algorithm approach, the entire target capture process consists of the following stages:

Stage 1: Target search. UAVs move randomly within a dynamic 3D environment to search for targets, considering collision avoidance during the search process.

Stage 2: Disseminate target information. When the UAV r_i^{UAV} $(i = 1.2, \ldots, n)$ finds the target T, the target information is obtained by the UAV. As a leader, r_i^{UAV} who found T spread target information to neighboring UAVs.

Stage 3: Calculate the cost value. A UAV that obtains target information can calculate the cost value of itself against the target with the following equation [10]:

$$Cost\left(r_i^{UAV}, T\right) = \gamma F\left(p_{r_i^{UAV}} - p_T\right) + \epsilon G(D_i, w) \quad (23)$$

where

$$F\left(p_{r_i^{UAV}} - p_T\right) = k_1 \left|p_{r_i^{UAV}} - p_T\right| + k_2 rand\left[1.0, \left|p_{r_{r_i^{UAV}}} - p_T\right|\right] \quad (24)$$

$$\epsilon G(D_i, w) = k_3 \pi d_{i1}^2 + k_4 w + k_5 (d_{i2} - w) \quad (25)$$

$$\left|p_{r_i^{UAV}} - p_T\right| = \sqrt{(a)^2 + (b)^2 + (c)^2} \quad (26)$$

$$a = X_{r_i^{UAV}} - X_T,\ b = Y_{r_i^{UAV}} - Y_T,\ c = Z_{r_i^{UAV}} - Z_T$$

where Euclidean distance between UAV and target is represented by $\left|p_{r_i^{UAV}} - p_T\right|$. The detection radius of UAV is symbolized by d_{i_1}. A maximum speed of a UAV is denoted by d_{i_2}. A maximum speed of a target is expressed as w, and weighting constants are stated as k_1, k_2, k_3, k_4, k_5.

Stage 4: Select three neighboring UAVs. The neighboring UAV calculates the cost value by using (23). Based on this value, three UAVs with a minimum cost value will go towards the target.

Stage 5: Form a target formation-pursuit. When a neighboring UAV with a minimum cost value toward the target, the four UAVs around the target form a formation-pursuit of moving target and herd the target to coordinates $[0,0,5]$. Multi-UAVs also consider collision avoidance capabilities during this process.

The dynamic task allocation algorithm for one UAV is described in Algorithm-1. It should be noted that every UAV on a distributed system is equally important, so the algorithm is also the same.

D. Position-based Formation-pursuit Strategy

There are n UAVs that perform formation-pursuit. Each UAV tracks the desired position that is around a moving target. The current UAV position and the desired position of the i-th UAV is represented by $\boldsymbol{p}_i = [X_i, Y_i. Z_i]^{\mathrm{T}}$ and $\boldsymbol{p}_{ref} = \left[X_{ref}, Y_{ref}, Z_{ref}\right]^{\mathrm{T}}$. The desired position can be seen in Fig. 6, where the target position T becomes the center of the formation-pursuit. In a formation-pursuit scenario, there must be points ($\boldsymbol{p}_{ref}$) to go around the target T being pursued.

The destination position consisting of four points is what will form a moving target formation-pursuit. To produce the desired position for each selected UAV to encircle the target can be searched using

$$\begin{aligned} X_{ref} &= X_T + \rho^* \sin k \cos m \\ Y_{ref} &= Y_T + \rho^* \sin k \sin m \\ Z_{ref} &= Z_T + \rho^* \cos k \end{aligned} \quad (27)$$

where $[X_T, Y_T, Z_T]^{\mathrm{T}}$ represents the target position, ρ^* indicates the encirclement radius, the angle between the UAV adjacent to the target on the horizontal line is m, and the angle on the vertical line is k.

The result $\left[X_{ref}, Y_{ref}, Z_{ref}\right]^{\mathrm{T}}$ of calculation with (27) then be an input for the tracking control in subsection B. The purpose of the formation-pursuit scenario based on this position is to reach $\boldsymbol{p}_i \rightarrow \boldsymbol{p}_{ref}$, for $i = 1,2, \ldots, n$.

E. Collision Avoidance

Collision avoidance is an essential ability of multi-UAV systems in a dynamic environment. In capturing a moving target, optimized APF is applied to avoid static obstacles (set of cylindrical buildings) and dynamic obstacles (other UAVs).

Optimized APF as global and local path planning is applied when UAV moves to capture the target and forms formation-pursuit.

Algorithm-1 Dynamic Task Allocation

1. r_i^{UAV} state, t_j, randomly;
2. Array: $T = \emptyset$;
3. **While** Capture task start
4. **if** $T = \emptyset$ **then**
5. Patrol and detect targets;
6. **if** r_i^{UAV} find target t_j **then**
7. $T \leftarrow t_j$;
8. Collect T information;
9. Broadcast T information;
10. Compute $Cost(r_i^{UAV}, t_j)$;
11. **if** receive target T information **then**
12. Compute $Cost(r_i^{UAV}, t_j)$;
13. **Else**
14. Choose r^{UAV} with $min\left(Cost(r_i^{UAV}, t_j)\right)$ move toward target T
15. Form formation-pursuit with selected r^{UAV}.

Then determined the equation attractive potential field [20]:

$$U_{att}(X) = \frac{1}{2} k_{att} (X - X_t)^2 \tag{28}$$

where k_{att} represents attractive potential field constant, X and X_t describe UAV and target position in the potential field. Attractive force $F_{att}(X)$ is a negative gradient of $U_{att}(X)$:

$$\begin{aligned} F_{att}(X) &= -\nabla U_{att}(X) \\ &= k_{att}(X_t - X) \end{aligned} \tag{29}$$

where the attractive force direction is along the line between the UAV and the target.

A local minimum problem that often occurs in APF is solved by modifying this algorithm through multiplying the original potential field repulsive function with the distance factor $(X - X_t)^n$ [15]. So that the repulsive potential field function is modified to:

$$U_{rep}(X) = \begin{cases} \frac{1}{2} k_{rep} \left(\frac{1}{\rho(X,X_o)} - \frac{1}{\rho_0}\right)^2 (X - X_t)^n, \rho(X,X_o) \le \rho_0 \\ 0, \qquad \rho(X,X_o) > \rho_0 \end{cases} \tag{30}$$

where k_{rep} represents repulsive potential field constant, $\rho(X, X_o)$ describes Euclidean distance between UAV and obstacle, ρ_0 indicates influence range of obstacles, the relative distance between UAV and target is $(X - X_t)^n = |(x - x_t)^n| + |(y - y_t)^n|$, and n represents a positive constant greater than zero. Repulsive force $F_{rep}(X)$ is the negative gradient of the U_{rep}:

$$F_{rep}(X) = -\nabla U_{rep}(X) = \begin{cases} F_{rep1}(X) + F_{rep2}(X), \ \rho(X,X_o) \le \rho_0 \\ 0, \qquad \rho(X,X_o) > \rho_0 \end{cases} \tag{31}$$

where

$$F_{rep1}(X) = k_{rep}\left(\frac{1}{\rho(X,X_o)} - \frac{1}{\rho_0}\right) \cdot \frac{1}{\rho^2(X,X_o)} \cdot (X - X_t)^n \cdot \frac{\partial \rho(X,X_o)}{\partial (X)} \tag{32}$$

$$F_{rep2}(X) = -\frac{n}{2} k_{rep}\left(\frac{1}{\rho(X,X_o)} - \frac{1}{\rho_0}\right)^2 \cdot (X - X_t)^{n-1} \cdot \frac{\partial (X - X_t)}{\partial (X)} \tag{33}$$

The repulsive potential field produced by other UAVs that are considered dynamic obstacles are:

$$U_{UAV}(i) = \begin{cases} \sum_{j=1}^{m} \frac{1}{2} k_{rep} \left(\frac{1}{\rho(X_i,X_j)} - \frac{1}{\rho_0}\right)^2 (X - X_t)^n, \rho(X_i,X_j) \le \rho_0 \\ 0, \qquad \rho(X_i,X_j) > \rho_0 \end{cases} \tag{34}$$

$$\rho(X_i, X_j) = \sqrt{(x_i - x_j)^2 + (y_i - y_j)^2 + (z_i - z_j)^2}$$

where $\rho(X_i, X_j)$ is Euclidean distance between i-th UAV and j-th UAV.

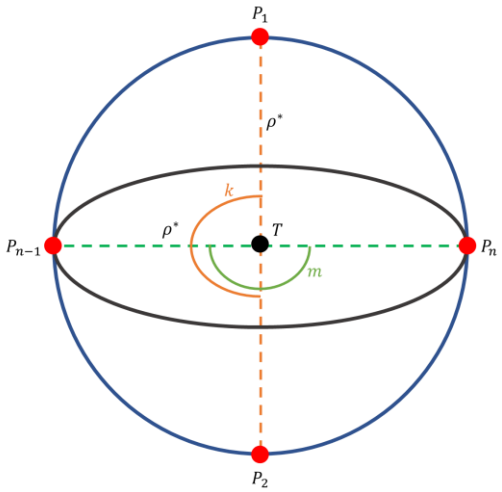

Fig. 6. Strategy of formation-pursuit a moving target using multi-UAVs

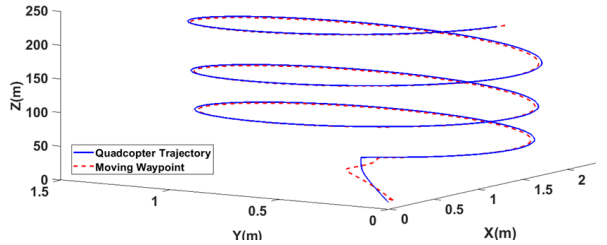

(a)

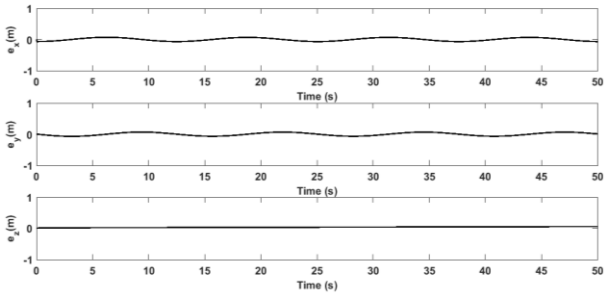

(b)

Fig. 7. Moving target tracking. (a) Trajectory tracking. (b) Position tracking error

TABLE III. PARAMETER OF TARGET CAPTURE SIMULATION

Parameter	Definition	Value
m_{UAV}	UAV mass (kg)	1
m_T	Target mass (kg)	1.2
ρ^*	Formation-pursuit radius (m)	3
d_{i1}	Detecting radius (m)	3
d_{i2}	Maximum velocity of UAV (m/s)	0 – 18
w_j	Maximum velocity of target (m/s)	0 – 16
k_{att}	Attractive gain coefficient	1
k_{rep}	Repulsive gain coefficient	30
ρ_0	Influence radius of the obstacle	1.2
n	Positive constant > 0	2

III. RESULTS AND DISCUSSION

The following tests were conducted to verify the performance of the proposed method.

A. Experiment of Tracking a Moving Target

The tracking controller was tested on a moving target by providing information such as a point of destination that can change at any time to the quadcopter. The tests were conducted to examine whether the proposed control method can be used to track a moving target. Inputs are given in the form of target positions (X_T, Y_T, Z_T), but the values of (X_T, Y_T, Z_T) are obtained from a function that causes the target position to change over time. The initial position value of the quadcopter was $[0, 0, 10]$ m. The trajectory of the moving target can be described using the equation below.

$$v_x = \frac{1}{2}\cos\left(\frac{t}{2}\right) \qquad X_t = X + k_x.v_x$$
$$v_y = \frac{1}{2}\sin\left(\frac{t}{2}\right) \qquad Y_t = Y + k_y.v_y$$
$$v_z = 2 + \frac{t}{10} \qquad Z_t = Z + k_z.v_z$$
$$t = i * Ts$$

where

X, Y, Z : Quadcopter position
X_t, Y_t, Z_t : Target position
v_x, v_y, v_z : Target velocity
k_x, k_y, k_z : Target constant (Value: $k_x = k_y = 1.4,\ k_z = 0.015$)
i : i-th iteration
T_s : Time sampling (Value: 0.01 seconds)

TABLE IV. INITIAL POSITION OF SEARCHER UAVS, TARGET, AND OBSTACLES

Subject Name	X (m)	Y (m)	Z (m)	Radius (m)
UAV 1	73.31	144.65	78.39	-
UAV 2	155.60	181.24	2.00	-
UAV 3	0.14	106.04	37.38	-
UAV 4	39.12	183.61	81.83	-
UAV 5	69.14	155.68	59.72	-
UAV 6	94.98	144.27	25.54	-
UAV 7	11.85	162.94	68.06	-
UAV 8	68.59	94.64	67.79	-
Target 1	29.31	144.83	9.94	-
Target 2	191.43	147.49	33.53	-
Obstacle 1	30	30	15	5
Obstacle 2	100	50	20	7
Obstacle 3	140	140	35	4
Obstacle 4	50	100	30	6

According to Fig. 7. (a), the proposed control method can follow a moving target in a 3D environment well. Moreover, in Fig. 7. (b), the controller can achieve a steady-state error close to zero for tracking positions.

B. Experiment of Target Capturing

Target capture scenario testing was conducted to test whether the proposed combination of task allocation, formation-pursuit, and collision avoidance is feasible and effective. The parameters used to test the entire target capture process can be seen in Table III.

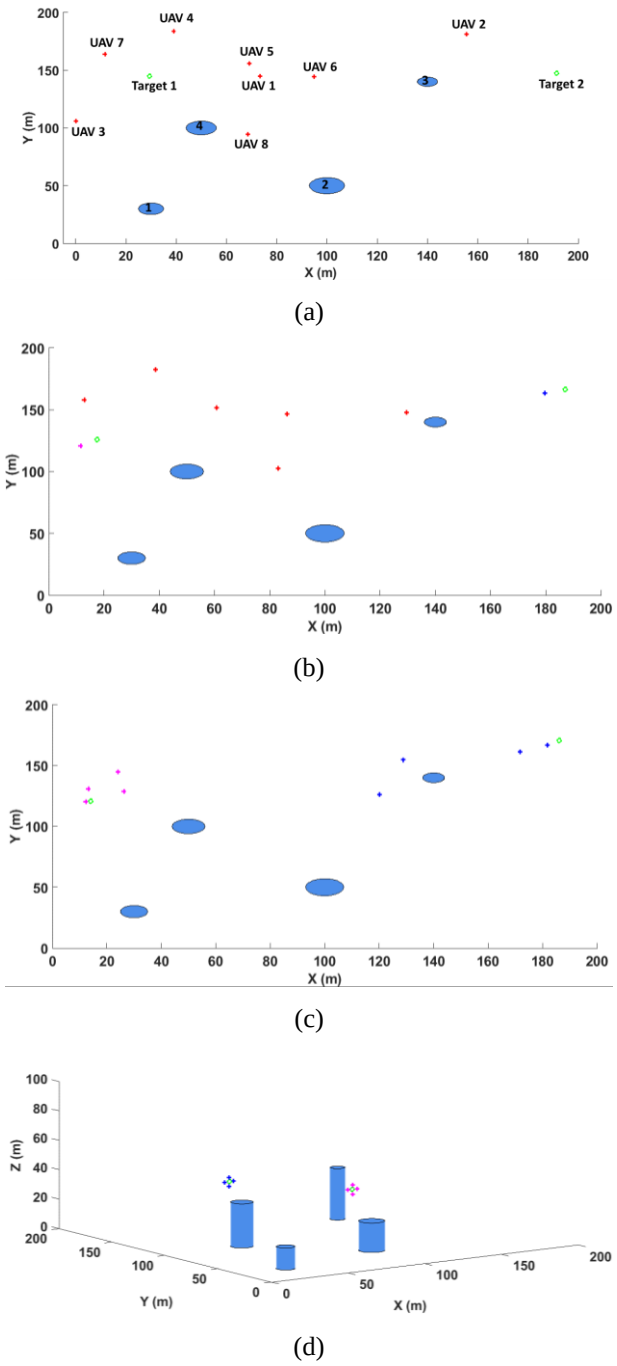

Fig. 8. Simulation of dynamic task allocation algorithm. (a) Initial position. (b-c) Target capture process. (d) Forming formation-pursuit of a target.

Testing the combination of task allocation, formation-pursuit, and collision avoidance in this experiment shows the combination method's performance if a target capture scenario consists of two UAVs as targets and eight searcher UAVs that move randomly and fly in a dynamic 3D environment. The initial position of the searcher UAVs, targets, and obstacles can be seen in Table IV.

As shown in Fig. 8. (a), the target and searcher UAVs moved with a random initial position. In Fig. 8. (b-c), searcher UAVs are patrolled to find targets within their detection radius. The UAV searcher who found a target became the temporary leader, as displayed in Fig. 8. (b). The target 1 and target 2 were marked with purple and blue, respectively. Then the leader will spread the target information to other UAV searchers while calculating his cost value against the target using (23). Next, the leader moved 3 meters above the target for do a formation-pursuit with radius ρ^*.

The neighboring UAV that received target information will calculate the cost value against the target, then three neighboring UAVs with a minimum cost value will be assigned to join the leader to form a formation-pursuit target. As shown in Fig. 8. (c), the searcher UAVs assigned to encircle the first target are UAVs 3, 4, 5, and 7, with a total cost value of 913.55, which is the minimum value of the total cost for the first target. As for the second target, four UAVs surrounded the target were UAVs 1, 2, 6, and 8, with a total cost of 1,218.1. Fig. 8. (d) shows that all searcher UAVs were successfully allocated to each target according to the minimum cost value, where four searcher UAVs must surround one target in formation-pursuit.

From the security side, this experiment was carried out to ensure that during the process of searching, capturing, encircling, and escorting the target to the endpoint [0,0,5]. There was no collision between the searcher UAV and the target, cylindrical building, and other searcher UAVs. Based on Fig. 9, the smallest distance between the searcher UAV and the target is 1.94359 m at 115.85 seconds. After that, the distance between the searcher UAV and the target reaches an equilibrium point of 2.99 m at 123.82 seconds, which is very close to the given input value of the formation-pursuit radius (ρ^*).

Fig. 10 shows the entire distance between searcher UAVs moving in a 3D environment. The value that shows the smallest distance between searcher UAVs is 1.32957 m at 114.85 seconds which occurs between UAVs 6 and 7. The distance between searcher UAVs and the four cylindrical buildings is shown in Fig. 11, where the smallest distance is 1.60632 m. The entire target capture process was successfully carried out without collisions with targets, cylindrical buildings, and other search UAVs as shown in Fig. 9 - Fig. 11.

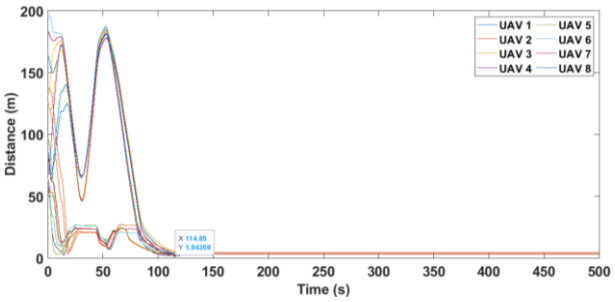

Fig. 9. Distance between searcher UAVs and target

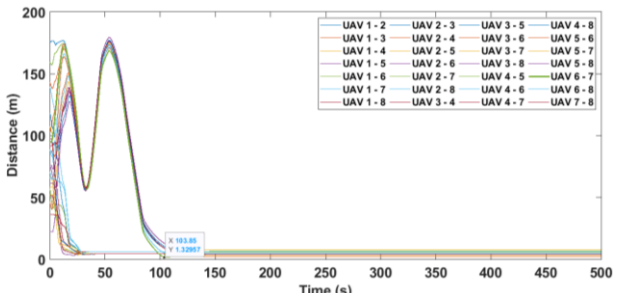

Fig. 10. Distance between searcher UAVs

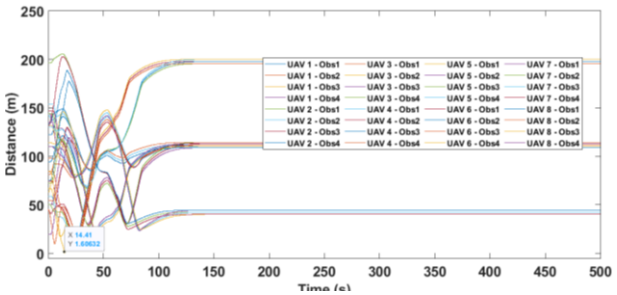

Fig. 11. Distance between searcher UAVs and obstacles

IV. Conclusion

This paper proposes an integrated moving target capture strategy for multi-UAVs by combining dynamic task allocation algorithm, fuzzy state feedback-based target tracking of formation-pursuit, and optimized APF-based collision avoidance.

The simulation results show that the smallest distance between UAVs of 1.32957 m, the closest distance between UAVs and target is 1.94359 m, and 1.60632 m for the shortest distance between UAV and obstacle. These values describe that the proposed cooperative control strategy can avoid collision with other UAVs, targets, and static obstacles during the target capture process. Last but not least, the proposed control strategy can allocate multi-UAVs to several moving targets.

Further research is needed to combine different platforms, such as an unmanned aerial vehicle (UAV) and unmanned ground vehicle (UGV), to study the allocation of more complex tasks in the process of capturing a moving target in the air and on the ground.

References

[1] Y. Fu, X. Wang, L. Huan, and H. Zhu, "Multi-UAV formation control method based on modified artificial physics," in Proc. *2016 Chinese Control and Decision Conference* (CCDC), pp. 2523-2529, 2016, doi: 10.1109/CCDC.2016.7531409.

[2] R. Xue and G. Cai, "Formation flight control of multi-UAV system with communication constraints," *Journal of Aerospace Technology and Management*, vol. 8, no. 2, pp. 203-210, 2016, doi: 10.5028/jatm.v8i2.608.

[3] A. Franchi, P. Stegagno, and G. Oriolo, "Decentralized multi-robot encirclement of a 3D target with guaranteed collision avoidance," *Autonomous Robots*, vol. 40, no. 2, 2016, doi: 10.1007/s10514-015-9450-3.

[4] S. Martin, "Multi-agent flocking under topological interactions," *Systems and Control Letters*, vol. 69, no. 1, 2014, doi: 10.1016/j.sysconle.2014.04.004.

[5] M. Rabah, A. Rohan, Y. J. Han, and S. H. Kim, "Design of fuzzy-PID controller for quadcopter trajectory-tracking," *International Journal of Fuzzy Logic and Intelligent Systems*, vol. 18, no. 3, 2018, doi: 10.5391/IJFIS.2018.18.3.204.

[6] M. H. Lee and S. Yeom, "Detection and tracking of multiple moving vehicles with a UAV," *International Journal of Fuzzy Logic and Intelligent Systems*, vol. 18, no. 3, 2018, doi: 10.5391/IJFIS.2018.18.3.182.

[7] R. Opromolla, G. Fasano, and D. Accardo, "A vision-based approach to uav detection and tracking in cooperative applications," *Sensors (Switzerland)*, vol. 18, no. 10, 2018, doi: 10.3390/s18103391.

[8] T. K. Venugopalan, K. Subramanian, and S. Sundaram, "Multi-UAV task allocation: A team-based approach," 2015. doi: 10.1109/SSCI.2015.17.

[9] H. A. Kurdi *et al.*, "Autonomous task allocation for multi-UAV systems based on the locust elastic behavior," *Applied Soft Computing Journal*, vol. 71, 2018. doi: 10.1016/j.asoc.2018.06.006.

[10] J. Ma, W. Yao, W. Dai, H. Lu, J. Xiao, and Z. Zheng, "Cooperative Encirclement Control for a Group of Targets by Decentralized Robots with Collision Avoidance," in Proc. *2018 Chinese Control Conference*, pp. 6848-6853, July 2018. doi: 10.23919/ChiCC.2018.8483768.

[11] K. S. Lee, M. Ovinis, T. Nagarajan, R. Seulin, and O. Morel, "Autonomous patrol and surveillance system using unmanned aerial vehicles," in Proc. *2015 IEEE 15th International Conference on Environment and Electrical Engineering* (EEEIC), June 2015. doi: 10.1109/EEEIC.2015.7165356.

[12] N. Nigam, "The multiple unmanned Air Vehicle persistent surveillance problem: A review," *Machines*, vol. 2, no. 1. 2014. doi: 10.3390/machines2010013.

[13] A. T. Hafez, M. Iskandarani, S. N. Givigi, S. Yousefi, and A. Beaulieu, "UAVs in formation and dynamic encirclement via Model Predictive Control," in Proc. *IFAC Proceedings Volumes (IFAC-PapersOnline)*, 2014, vol. 19. doi: 10.3182/20140824-6-za-1003.00890.

[14] A. T. Hafez, A. J. Marasco, S. N. Givigi, M. Iskandarani, S. Yousefi, and C. A. Rabbath, "Solving Multi-UAV Dynamic Encirclement via Model Predictive Control," *IEEE Trans. Control Syst. Technol.*, vol. 23, no. 6, pp. 2251-2265, 2015, doi: 10.1109/TCST.2015.2411632.

[15] J. Sun, J. Tang, and S. Lao, "Collision Avoidance for Cooperative UAVs with Optimized Artificial Potential Field Algorithm," *IEEE Access*, vol. 5, 2017, doi: 10.1109/ACCESS.2017.2746752.

[16] E. Ferrera, A. Alcántara, J. Capitán, A. R. Castaño, P. J. Marrón, and A. Ollero, "Decentralized 3D Collision Avoidance for Multiple UAVs in Outdoor Environments," *Sensors (Basel)*, vol. 18, no. 12, 2018, doi: 10.3390/s18124101.

[17] T. Agustinah, F. Isdaryani, and M. Nuh, "Tracking control of quadrotor using static output feedback with modified command-generator tracker," *International*

Review of Automatic Control, vol. 9, no. 4, 2016, doi: 10.15866/ireaco.v9i4.9431.

[18] Quanser, "QDrone Product Data Sheet v1.3," 2018, [Online]. Available: https://www.quanser.com/wp-content/uploads/2018/02/QDrone-Product-Data-Sheet-v1.3.pdf

[19] Y. Jiang, "A Survey of Task Allocation and Load Balancing in Distributed Systems," *IEEE Trans. Parallel and Distributed Systems*, vol. 27, no. 2, 2016, doi: 10.1109/TPDS.2015.2407900.

[20] O. Khatib, "Real-Time Obstacle Avoidance For Manipulators And Mobile Robots.," *International Journal of Robotics Research*, vol. 5, no. 1, 1986, doi: 10.1177/027836498600500106.